Strain-Induced Crystallization of *cis*-1,4-Polybutadiene Containing Dispersed 1,2-Polybutadiene Crystalline Particles

N. NAKAJIMA* and Y. YAMAGUCHI†

Institute of Polymer Engineering, The University of Akron, Akron, Ohio 44325-0301

SYNOPSIS

Some grades of *cis*-1,4-polybutadiene contain dispersed crystalline particles made up of a block copolymer having amorphous *cis*-1,4- and crystalline 1,2 blocks. The particles are known to enhance the strain-induced crystallization of *cis*-1,4 matrix rubber. The deformational behavior was examined by dynamic shear measurements at small deformation and tensile stress–strain measurements at large deformation. In the shear measurements (linear behavior), the temperature dependence of the shift factor in the time-temperature superposition has been evaluated. The higher temperature dependence was observed for the lower crystalline particle content and higher degree of branching of the matrix rubber. The presence of the crystalline particles resulted in the viscosity enhancement like that expected from the dispersed particles. In the tensile measurements (nonlinear behavior), the rubbers showed strain softening. The higher degree of strain softening was observed for the higher amount of the crystalline particles and lower degree of branching. The strain softening is a result of the crystalline particles facilitating the elongation. Because these particles possess the branches which are *cis*-1,4 chains of the block copolymer, the branches are lubricating the system during the stretching. The length of the branches must be short enough so as to produce no significant entanglement constraint. This observation is in accord with the previous one that a relatively long branch gives strain hardening, whereas a relatively short branch gives strain softening. The strain softening was found to enhance the strain-induced crystallization. This conclusion is opposite to what one might expect from the entanglement constraints by the long branches, forcing the orientation of the chains, and thus enhancing the strain-induced crystallization. © 1996 John Wiley & Sons, Inc.

INTRODUCTION

A major application of *cis*-1,4-polybutadiene is tire. The rubber improves wear resistance, rolling resistance, and flexibility at low temperature. It is usually used with other rubbers, such as NR or SBR because it does not have a good processability, flex-crack resistance, and green strength. In order to overcome the weakness, *cis*-1,4-polybutadiene (UBEPOL VCR) containing particles of a highly crystalline syndiotactic 1,2-polybutadiene have been developed.[1] The particles are made up of block copolymer of *cis*-1,4- and 1,2-polybutadiene. The crystalline particles are effective for producing the strain-induced crystallization[1] of the rubber matrix; as a result, the weaknesses mentioned above have been overcome. The influence of such crystalline particles on rheological properties is our particular interest here. Even though *cis*-1,4-polybutadiene is known to crystallize, there is very little literature on strain-induced crystallization. The study is usually conducted with vulcanized specimens; in one study, prestretched specimens were cooled to crystallize below the normal crystallization temperature[2]; in the

Based on a paper presented at the International Rubber Conference, Kobe, Japan, October 24–27, 1995.

* To whom correspondence should be addressed.

† Present address: Yokohama Rubber Co., 1-2 Oiwake, Hiratsuka 254, Japan.

Journal of Applied Polymer Science, Vol. 62, 2329–2339 (1996)
 CCC 0021-8995/96/132329-11

Table I Samples

Sample	M_w[a], 10^{-4}	M_n[a], 10^{-4}	M_w/M_n[a]	SPB[b] (wt %)	MV[c]
VCR309[d]	45.9	17.1	2.7	9	39
VCR412[d]	45.1	18.4	2.5	12	45
VCR617[d]	46.2	17.6	2.6	17	63
VCR512[d]	44.2	15.5	2.9	12	43

Data supplied by the manufacturer.

[a] Data by GPC; molecular weights are not absolute but relative values based on the hydrodynamically equivalent volume of polystyrene standards. The data represent the matrix polymer only.

[b] The amount of syndiotactic 1,2-polybutadiene crystalline particle.

[c] Moony viscosity.

[d] Registered trademark of UBE Industries.

other study, the equilibrium stress–strain measurements were performed above the melting temperature.[3]

Our interest is in the unvulcanized specimens and in the nonequilibrium stress-strain behavior at the ambient temperature. In addition to the effect of the crystalline particles, the effect of long branching of the matrix rubber is also examined.

The conventional methods of the rheological characterization are the uses of Moony Index and the steady-state shear measurements. However, the information obtained from these methods are not adequate for understanding the processability because processing of elastomers involves transient and large deformation in shear and elongation.

In the previous work,[4] the effect of long branching in *cis*-1,4-polybutadienes on the deformational behavior was investigated. Oscillatory shear measurements at small deformation and tensile stress-strain measurements at large deformation were performed. In the former, the temperature dependence of the shift factor in the time-temperature superposion was found to relate to the degree of branching from the dilute solution viscosity. In the elongational measurements, some rubbers exhibited strain hardening, others strain softening, and, in some case, neither hardening nor softening. The differences were not related to the degree of branching observed in the dilute solution viscosity. The strain softening was attributed to the relative shortness of the branches, whereas the strain hardening was attributed to the relatively long branches. Comparing the shear and elongation data indicated a structure development upon stretching, the fact which was interpreted to be the strain-induced crystallization. The similar

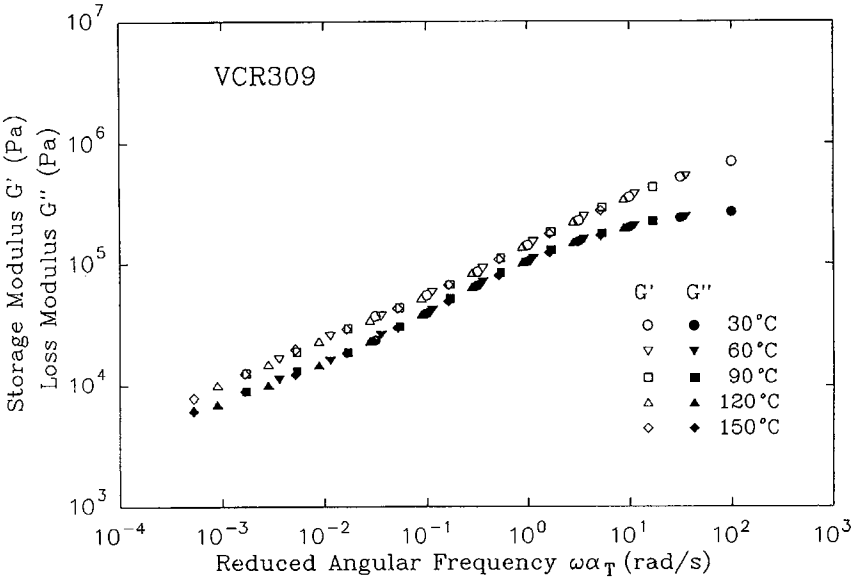

Figure 1 Master curves of storage and loss modulus of VCR309. Reference temperature is 30°C.

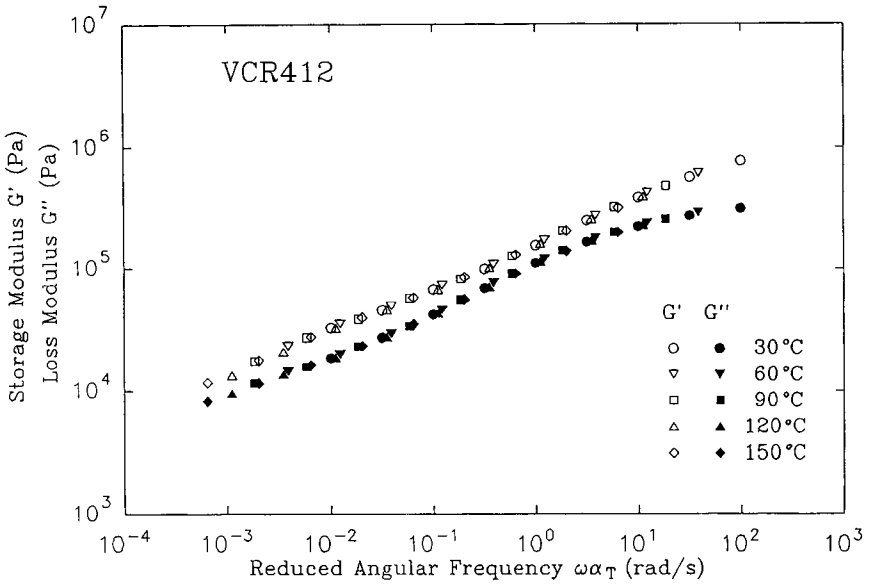

Figure 2 Master curves of storage and loss modulus of VCR412. Reference temperature is 30°C.

methods of the deformational analyses are used in this study.

Viscoelastic Characterization Methods

The oscillatory shear data are presented as the storage modulus G' and the loss modulus G'', i.e., a plot of log G''–log G'. From our previous experience, we know that a degree of branching may be assessed from the relative position of the curve.[5]

The tensile stress–strain data may be presented with the modulus E as a function of strain ε and time t,[6]

$$E(\varepsilon, t) = \sigma/\varepsilon \tag{1}$$

where σ is the true stress based on the cross-sectional area of a deformed specimen, and ε is related to the extension ratio, and α as

$$\varepsilon = \alpha - 1 \tag{2}$$

When the experiment is performed at a constant deformation rate $\dot{\varepsilon}$, the time and strain are related as

$$t = \varepsilon/\dot{\varepsilon} \tag{3}$$

With some rubbers, a particular form of the strain-time correspondence principle is applicable,[7] and the modulus E is a function of reduced time αt, as follows:

$$\sigma/\varepsilon = E(\alpha t) \tag{4}$$

where the strain-shift factor α is the extension ratio. Henceforth, eq. (4) is referred as the strain–time correspondence. When eq. (4) is applicable, the tensile stress–strain results obtained at different deformation rates form a master curve.

The tensile modulus may be converted into an equivalent of the shear viscosity η_T with $(1/\alpha t)$ being the reduced deformation rate

$$3\eta_T = E(\alpha t)\alpha t \tag{5}$$

The factor 3 relates shear and elongation behavior for Poisson's ratio of 0.5. When eq. (4) results in the linearization of nonlinear data, η_T may be compared to the absolute value of the complex viscosity, $|\eta^*|$, as follows:

$$\eta_T = |\eta^*| \tag{6}$$

the viscosities being taken at equal value of the frequency ω, rad/s, and the rate $1/\alpha t$, s^{-1}.

Gel-free elastomers and elastomers containing microgel (a crosslinked particle) obey the above reduction scheme. However, elastomers containing macrogel (extensively branched molecule) do not obey the relation, exhibiting strain hardening. Subsequently, modulus shift is applied to obtain a mas-

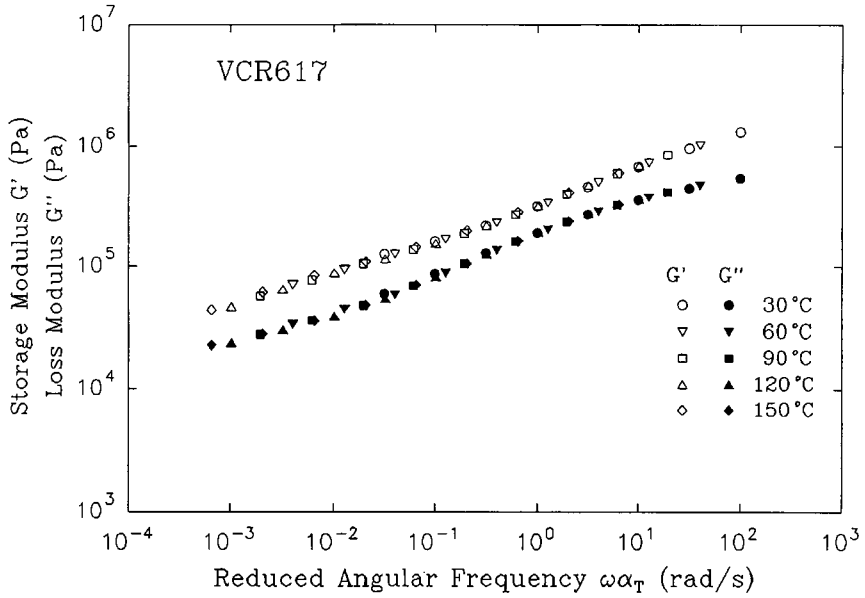

Figure 3 Master curves of storage and loss modulus of VCR617. Reference temperature is 30°C.

ter curve. Then, the modulus shift factor $\Gamma(\alpha)$ is a measure of the strain hardening[7]

$$3\eta_T = E(\alpha t)\alpha t/\Gamma(\alpha) \quad (7)$$

When there is a strain-induced crystallization or polar association upon stretching, a relation, $|\eta^*| < \eta_T$, was found.

EXPERIMENTAL

Samples

The samples were four commercial polybutadienes (UBEPOL VCR) produced by UBE Industries (Table I). These rubbers contain crystalline particles of syndiotactic 1,2-polybutadiene in the matrix polymer of *cis*-1,4-polybutadiene. The crystalline particle

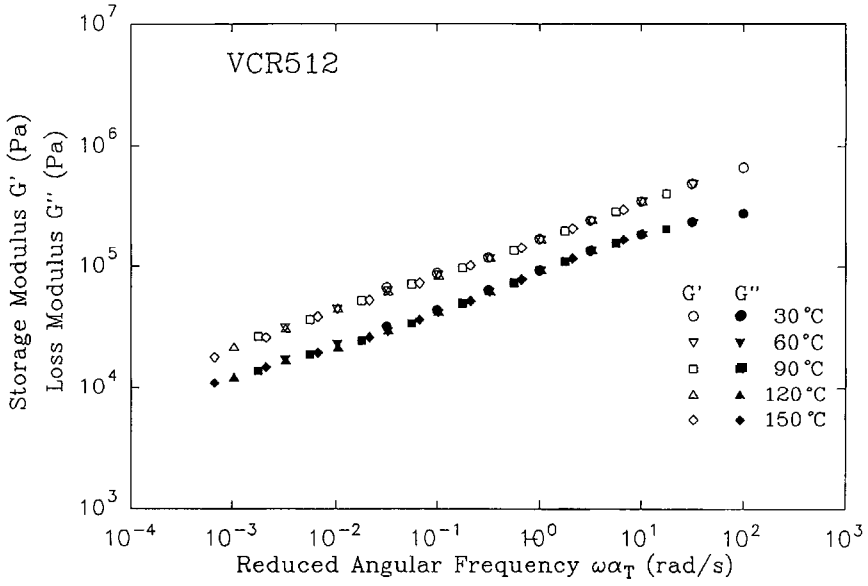

Figure 4 Master curves of storage and loss modulus of VCR512. Reference temperature is 30°C.

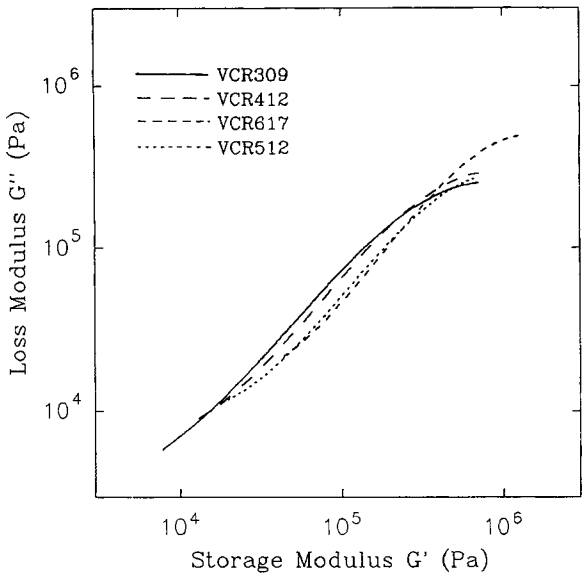

Figure 5 Comparison of log G'' versus log G' curves.

is composed of block copolymers of *cis*-1,4/1,2-vinyl butadiene.[1] It has 80% crystallinity in the 1,2-polybutadiene domain and a melting point of 204°C. The rubbers of VCR309, VCR412, and VCR617 have different amounts of crystalline particles in the same matrix polymer. Although not shown in Table I, VCR512 has a different matrix polymer that is more branched than the matrix of other samples.

The sheets of gum rubbers were prepared by pressing at 140°C for 10 min. Oscillatory shear specimens were cut from the sheets as a disc of 25 mm diameter, and tensile specimens were cut with ASTM D412 dumbbell die *C*.

Instruments

The oscillatory shear measurements were performed with a Rheometrics mechanical spectrometer RMS800 with parallel plates. The angular frequency range was from 10^{-2} to 10^2 rad/s. The samples were tested at 30, 60, 90, 120, and 150°C. In addition to the calibration specified by the instrument manufacturer, a standard silicon rubber (SE30; General Electric Company) was used every time to double check the calibration. The frequency sweep was made from the lowest to the highest and then reversed to the lowest frequency. The data at the lowest frequency should reproduce, if there is no degradation during the measurements.

Tensile tests were performed with a Monsanto Tensometer 500. The strip chart recorder recorded force against time. The force was measured with a 0.45 kg load cell. The extent of deformation was measured by recording with a video camera. An extensometer was not used because the samples were not strong enough to hold it. The samples were held with plastic grips having relatively loose springs in order to prevent breaking at the grips. The tests were performed at the room temperature with strain rates of 0.003, 0.011, 0.038, 0.087, and 0.118 s^{-1}.

RESULTS AND DISCUSSION

Oscillatory Shear Measurements

The results of time-temperature superposition are shown in Figures 1 through 4, where all the data were reduced to 30°C. The time–temperature superposition was performed in the following sequence. First, tan δ data were plotted against log ω. The superposition involves shifts in log ω axis only, because any modulus shift in G' and G'' cancels out. From this procedure, the time-shift factor α_T was evaluated. Next, log $|G^*|$ data were plotted against log $\omega\alpha_T$. From these plots, the modulus shift factor β_T was evaluated.

Table II Shift Factor, α_T and β_T

		Temperature (°C)				
	Sample	30	60	90	120	150
α_T	VCR309	1	0.360	0.171	0.089	0.052
α_T	VCR412	1	0.388	0.186	0.111	0.064
α_T	VCR617	1	0.404	0.195	0.102	0.065
α_T	VCR512	1	0.325	0.178	0.104	0.067
β_T	VCR309	1	0.906	0.830	0.731	0.665
β_T	VCR412	1	0.971	0.889	0.839	0.793
β_T	VCR617	1	1	1	0.879	0.855
β_T	VCR512	1	0.859	0.849	0.774	0.714
β_T	$\rho_0 T_0/\rho T$	1	0.910	0.835	0.771	0.716

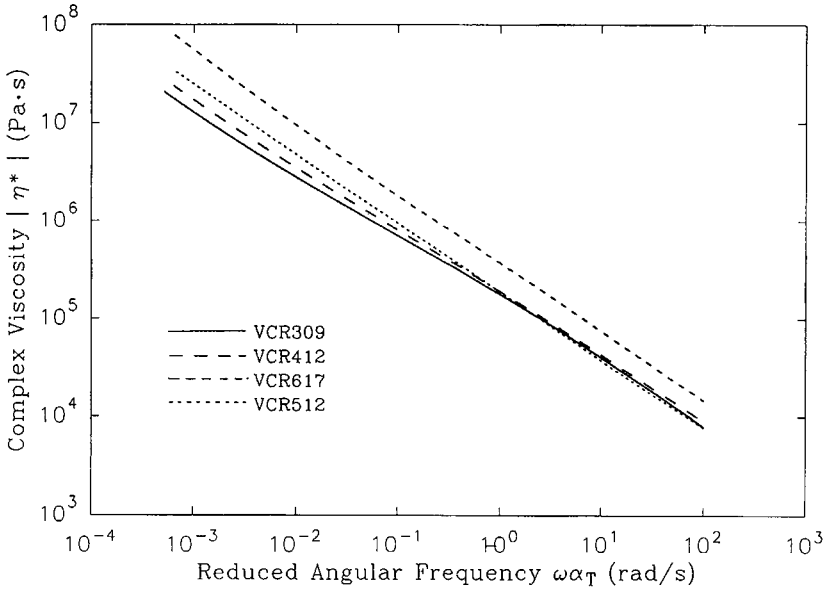

Figure 6 Comparison of master curves of complex viscosity. Reference temperature is 30°C.

The extent of the time shift was rather small; for the data of 30–150°C, the frequency range was extended only about one decade to lower frequencies. This is because the glass transition temperature of *cis*-polybutadiene is very low, i.e., −110°C. All master curves approach the plateau region at the higher frequencies. However, these curves do not show the cross over of G' and G''. They are almost parallel to

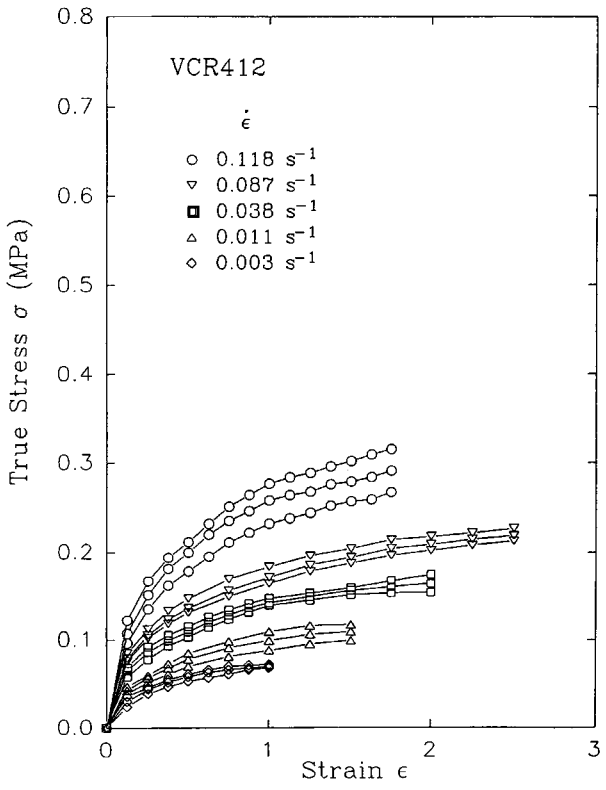

Figure 7 Tensile stress–strain curves of VCR412.

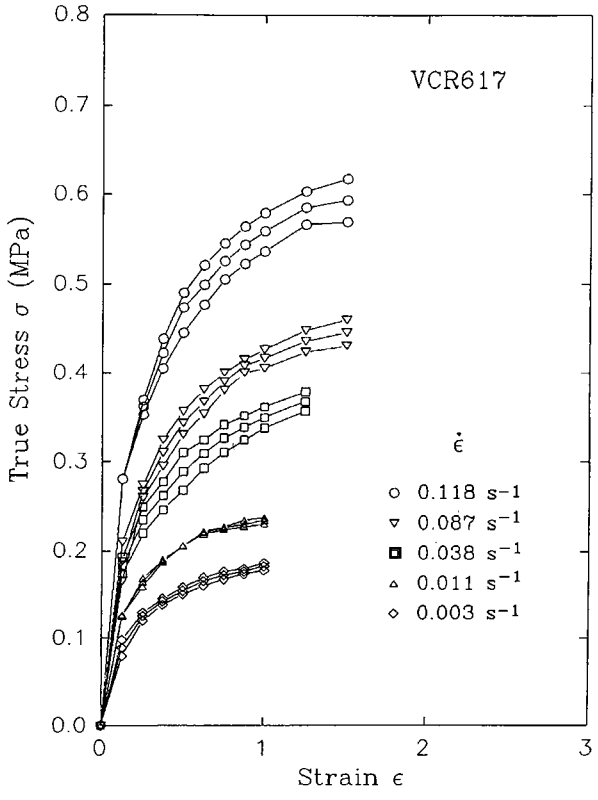

Figure 8 Tensile stress–strain curves of VCR617.

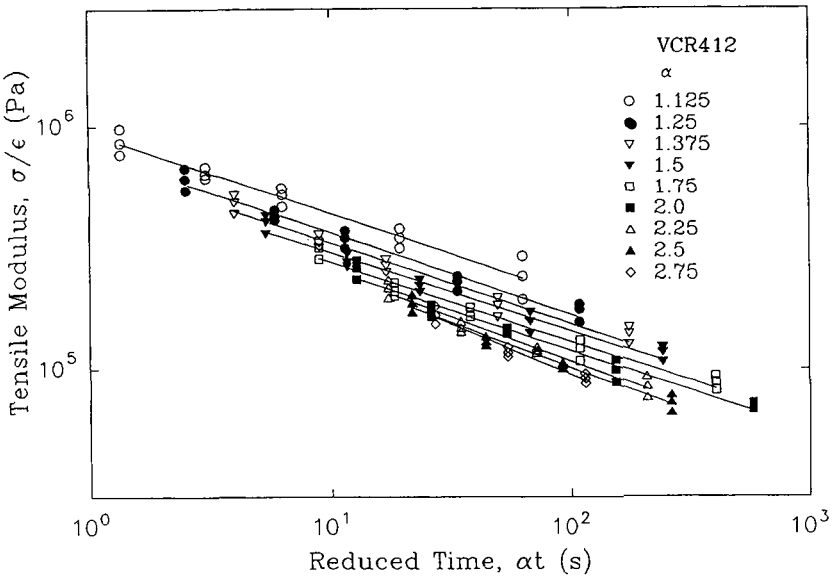

Figure 9 Tensile modulus as a function of reduced time at fixed extension ratios for VCR412.

each other. This is because of the presence of the crystalline particles and branching in the matrix polymer.

Figure 5 shows log G'' versus log G' plot for the all four rubbers. The curves shift to the right with the increasing amount of the crystalline particles. This indicates that the rubber becomes more elastic in the presence of the particles. The curve of VCR512 lies at the right side of that of VCR412 because the matrix polymer of the former is more branched than the matrix of the latter.

The values of the shift factors, α_T and β_T are given in Table II. The α_Ts are sample dependent, and VCR309, which has the least amount of the crystalline particles, shows the highest temperature dependence among the rubbers having same matrix polymer. The rubber having more branched matrix, VCR512, shows somewhat higher temperature dependence than that of VCR412. However, the differences of α_T diminish at the higher temperature. The observed values of β_T (Table II) are comparable to the values of $\rho_0 T_0/\rho T$. The temperature depen-

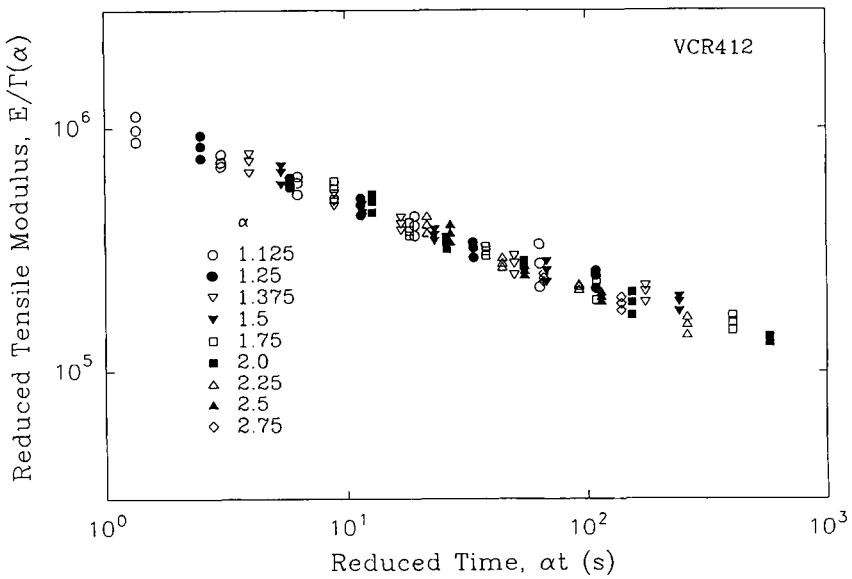

Figure 10 Reduced tensile modulus as a function of reduced time for VCR412.

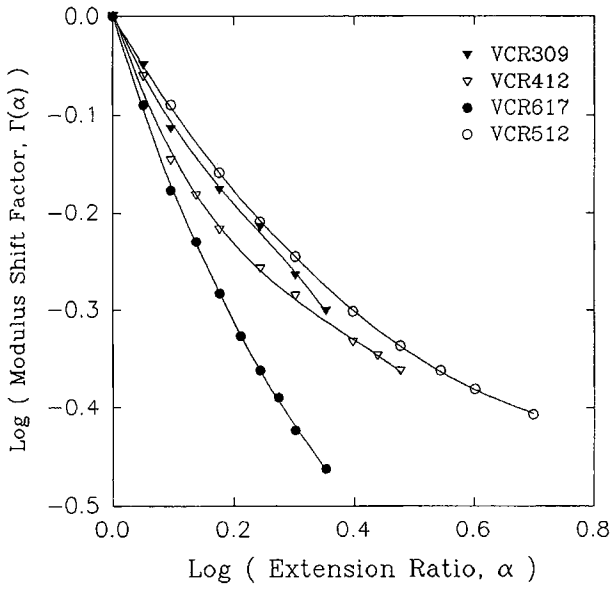

Figure 11 Modulus shift factor as a function of extension ratio.

dence of β_T decreases with the increasing particles content, and it almost disappears for VCR617 between 30 and 90°C. This may be the result of the difference in the thermal expansion coefficients of the matrix rubber and the crystalline particle.

Figure 6 shows the absolute values of complex viscosity $|\eta^*|$ of the rubbers at 30°C. As observed in many commercial rubbers, these do not show the Newtonian region within the observed time scale because of their high molecular weight, broad molecular weight distribution, branching, and the presence of the particles. Among VCR309, VCR412, and VCR617, the value of $|\eta^*|$ is higher for larger amount of the crystalline particles. At low frequencies, viscosity enhancement increases with increasing amount of crystalline particles. This is like the effect of the dispersed particles on viscosity. At low frequencies, viscosity of VCR512 is higher than that of VCR412. As the frequency is increased, the curve of VCR512 cross over the curve of VCR412. This is the result of VCR512 having more extensive branching compared to VCR412.

Tensile Stress–Strain Measurements

Figures 7 and 8 show tensile stress-strain curves of VCR412 and VCR617 at various deformation rates. The stress σ is the true stress based on the deformed cross section. Reproducibility shown in the figures is less than ±15%. The modulus increases with increasing deformation rates. It is higher for the higher amount of the crystalline particles. The stress-strain curves of the other samples are similar to those shown in Figures 7 and 8.

Figure 9 shows the plots of tensile modulus $E(\alpha_t)$ against reduced time αt for VCR412, as was given by eq. (4). In this figure, the lines connect the data at a constant value of α. Instead of forming a master curve, the data systematically change with α. The deviation is in the direction of strain softening.

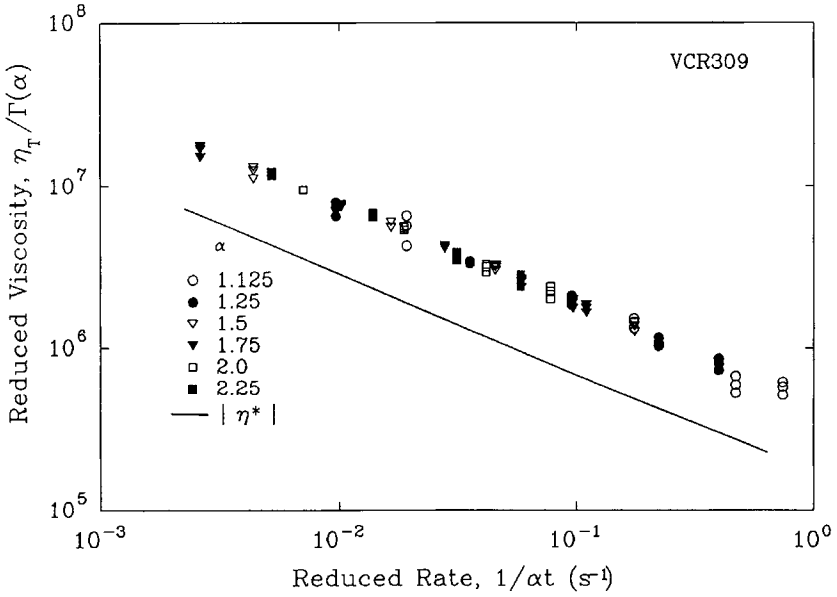

Figure 12 Comparison of shear complex viscosity with corresponding viscosity calculated from tensile data for VCR309.

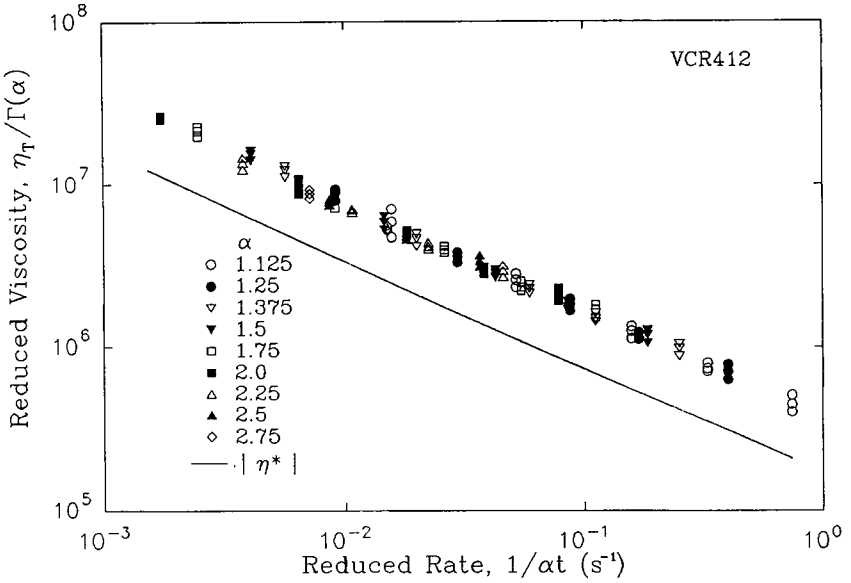

Figure 13 Comparison of shear complex viscosity with corresponding viscosity calculated from tensile data for VCR412.

When the modulus shift,[7] eq. (7) is applied, master curves are formed for all rubbers, like in Figure 10 for VCR412. Figure 11 shows the modulus shift $\Gamma(\alpha)$ as a function of extension ratio. The degree of the strain softening increases with increasing amount of the crystalline particles.

As mentioned before, the crystalline particle consists of a block copolymer of *cis*-1,4-polybutadiene and 1,2-polybutadiene, the latter providing a crystalline morphology. The *cis*-1,4 chains presumably cover the surface of the particles, compatibilizing the particles with the matrix rubber. A diffused boundary between the particle and the matrix was observed with TEM for an ultrathin section.[1] Therefore, the *cis*-1,4 chains are like branches spreading out of the surface of the particles. When the branches are not long enough to give the entanglement constraints, they facilitated stretching by

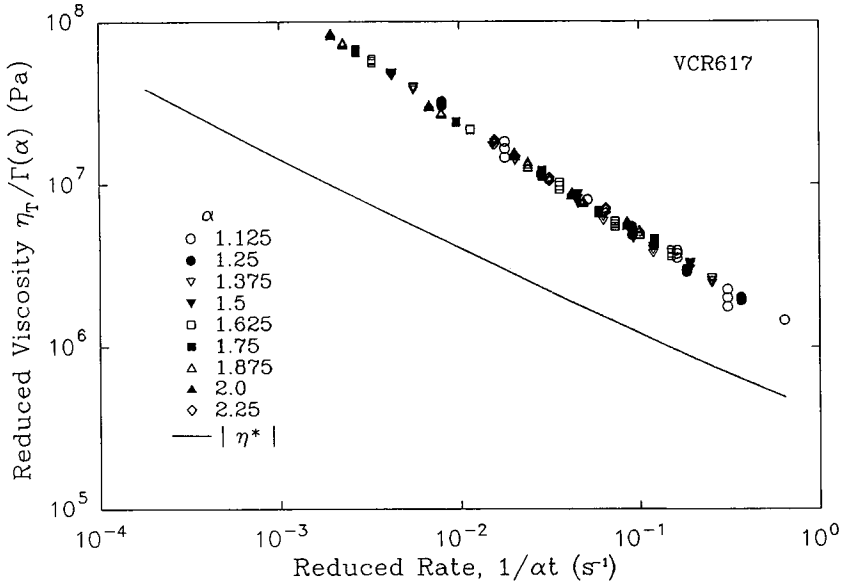

Figure 14 Comparison of shear complex viscosity with corresponding viscosity calculated from tensile data for VCR617.

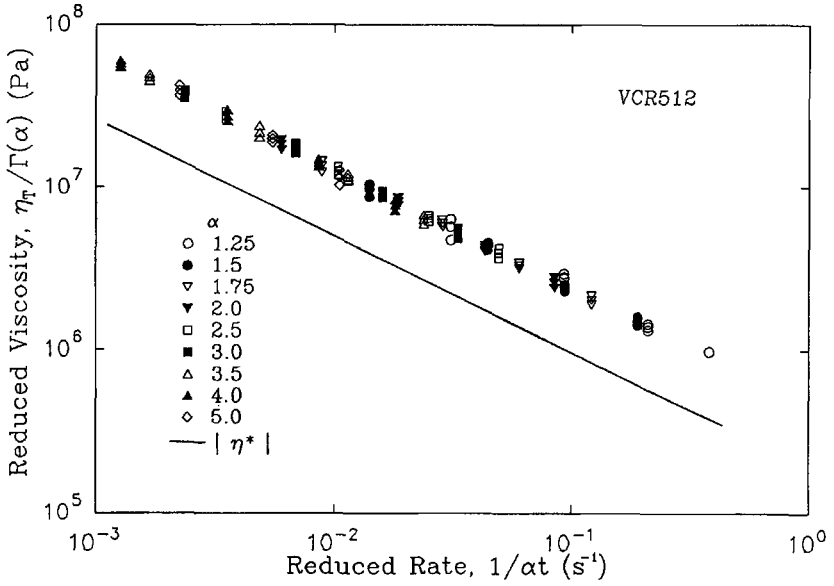

Figure 15 Comparison of shear complex viscosity with corresponding viscosity calculated from tensile data for VCR512.

lubrication. Because the crystalline particles are giving strain softening, the branches on the particles are not long enough to give the entanglement constraints. This is also evident since more particles give more strain softening.

Although VCR512 and VCR412 contain the same amount of the crystalline particles, the latter gives more strain softening than the former. The matrix polymer of VCR512 has longer branches than that of VCR412 such that the branching in the former is giving a constrained entanglement. The consequent strain-hardening tendency somewhat offsets the overall degree of the strain softening from the crystalline particles.

Figures 12 through 15 show comparisons between the complex viscosity $|\eta^*|$ and the equivalent of shear viscosity η_T, calculated from the tensile stress-strain data. The calculation of η_T includes the modulus shift. The curves of η_T are higher than curves of $|\eta^*|$ for all rubbers. This indicates the strain-induced crystallization of the matrix polymer at the large elongational deformation. The curves of η_T and $|\eta^*|$ for VCR309, VCR412, and VCR512 are almost parallel to each other. The curves for VCR617 are not parallel, and the difference becomes larger toward lower frequencies. This is because higher crystalline-particle content introduces higher strain-induced crystallization, and the crystallization is more significant at the large deformation, which corresponds to the lower frequency in this presentation.

In the previous study[4] as well as this study, the strain softening was found to facilitate the strain-induced crystallization. This is contrary to what one might expect from the constraint against elongation, forcing the orientation of the chains, and, thus, enhancing the crystallization. The exact mechanism of strain-induced crystallization requires a further study.

CONCLUSION

The rubbers containing more crystals or more branched matrix polymer are more elastic, i.e., possess a higher G' compared at the equal value of G''.

In the temperature dependence of the time shift factor in the time–temperature superposition, the higher temperature dependence was shown for the rubber containing less crystalline particles or having more branched matrix polymer.

The tensile measurements showed strain softening for all rubbers. The strain softening was larger for the rubber containing more crystalline particles and having less degree of long branching in matrix polymer. Because the branches on the particles are presumably not long enough to give constrained entanglements, the crystalline particles work as if they are surface-lubricated fillers.

A comparison of the complex shear viscosity $|\eta^*|$ and the viscosity calculated from tensile behavior η_T showed that η_T was higher than $|\eta^*|$. The differences between η_T and $|\eta^*|$ were larger for the higher amount of the crystalline particle. The disagreement between η_T and $|\eta^*|$ shows a structure

development upon stretching, a fact which is attributable to the strain-induced crystallization.

REFERENCES

1. M. Takayanagi, Paper presented to the 19th Annual Meeting of the International Institute of Synthetic Rubber Producers, Hong Kong, 1978.
2. D. Göritz and M. Kiss, *Rubber Chem. Technol.*, **59,** 40 (1986).
3. T.-K. Su and J. E. Mark, *Rubber Chem. Technol.*, **51,** 285 (1978).
4. N. Nakajima and Y. Yamaguchi, Paper presented at the Meeting of the Rubber Division, ASC, Philadelphia, May 2–5, 1995.
5. N. Nakajima and E. R. Harrell, *Current Topics in Polymer Science, Vol. II: Rheology and Polymer Processing/Multiphase Systems,* R. M. Ottenbrite, L. A. Utracki, and S. Inoue, Eds., Macmillan, New York, 1987, p. 149.
6. T. L. Smith, *Trans. Soc. Rheol.*, **6,** 61 (1962).
7. N. Nakajima, C. D. Huang, J. J. Scobbo Jr., and W. J. Shieh, *Rubber Chem. Technol.*, **62,** 343 (1989).

Received April 19, 1996
Accepted July 22, 1996